Fivefold increase of hydrogen uptake in MOF74 through linker decorations

C. A. Arter, S. Zuluaga, D. Harrison, E. Welchman, and T. Thonhauser

Phys. Rev. B **94**, 144105 — Published 21 October 2016

DOI: 10.1103/PhysRevB.94.144105

5-fold increase of hydrogen uptake in MOF74 through linker decorations

C. A. Arter, S. Zuluaga, D. Harrison, E. Welchman, and T. Thonhauser*
Department of Physics, Wake Forest University, Winston-Salem, NC 27109, USA
(Dated: September 30, 2016)

We present *ab initio* results for linker decorations in Mg-MOF74—i.e. attaching various metals $\mathcal{M}$ = Li, Na, K, Sc, Cr, Mn, Fe, Ni, Cu, Zn, Rb, Pd, Ag, and Pt near the ring of the linker—creating new strong adsorption sites and thus maximizing small molecule uptake. We find that in most cases these decorations influence the overall form and structure of Mg-MOF74 only marginally. After the initial screening we chose metals that bind favorably to the linker and further investigate adsorption of H_2, CO_2, and H_2O for $\mathcal{M}$ = Li, Na, K, and Sc. For the case of H_2 we show that up to 24 additional guest molecules can be adsorbed in the MOF unit cell, with binding energies comparable to the original open-metal sites at the six corners of the channel. This leads to a 5-fold increase of the molecule uptake in Mg-MOF74, with tremendous impact on many applications in general and hydrogen storage in particular—where the gravimetric hydrogen density increases from 1.63 mass% to 7.28 mass% and the volumetric density from 15.10 g H_2 L^{-1} to 75.50 g H_2 L^{-1}.

PACS numbers: 71.15.Mb, 31.15.ej, 81.05.Rm

I. INTRODUCTION

With the growing interest in gas storage, separation, and sensing, metal organic framework (MOF) materials have become the focus of intense research, as their nanoporous nature and extraordinary affinity for adsorption of small molecules make them ideal for these technologically important applications.[1–3] In addition, their modular building-block nature allows for an unprecedented tune-ability, which can be utilized to tailor their properties to desired needs, with remarkable success.[4–10] One property of much interest for many applications such as gas separation and storage is the small-molecule uptake of MOFs. Although MOFs have been declared DOE's top priority at its *2012 Hydrogen and Fuel Cells Program Annual Review Meeting* due to their favorable H_2 desorption characteristics,[11] unfortunately, their gravimetric H_2 storage density lags behind other classes of materials.[12] To fully utilize the potential of MOFs for many applications in general—and for hydrogen storage in particular—it is thus highly desirable to maximize their small-molecule uptake and storage capacity.

In this letter, we focus on one particular MOF, i.e. MOF74 [$\mathcal{X}_2$(dobdc), $\mathcal{X}$ = Mg^{2+}, Zn^{2+}, Ni^{2+}, Co^{2+}, and dobdc = 2,5-dihydroxybenzenedicarboxylic acid], and show that the small-molecule uptake can be significantly increased by a simple linker decoration. To maximize the gravimetric storage density, we focus on the lightest representative of the isostructural series $\mathcal{X}$-MOF74, i.e. Mg-MOF74, which exhibits hexagonal channels with under-coordinated open-metal sites at the corners, forming the six main adsorption sites in the unit cell (see Fig. 1). Although secondary adsorption sites exist near the linker,[13] they typically bind the guest molecules much more weakly. We thus seek to introduce additional adsorption sites, comparable in binding strength to the original under-coordinated open-metal sites. To this end, we consider two different linker decorations, which we call *center* (*c*) and *outside* (*o*), where we attach metal atoms $\mathcal{M}$ near the ring of the 2,5-dihydroxybenzenedicarboxylic acid linker of MOF74, as depicted in Fig. 1. These decorations were motivated by other organometallic compounds and metalloligands,[14–19] as well as successful modifications in other MOFs.[20–32] Our selection of metals $\mathcal{M}$ = Li, Na, K, Sc, Cr, Mn, Fe, Ni, Cu, Zn, Rb, Pd, Ag, and Pt was influenced by previous studies that investigate metal interactions with benzene.[33–37] In this paper, we show that a number of these metals favorably bind to the linker and, in turn, form new and strong adsorption sites that can bind several additional guest molecules.

Synthesizing our proposed linker decorations may be possible with molecular beam methods that utilize a combination of laser-vaporization methods and flow-tube reactors, which have been successful in creating very similar transition-metal benzene complexes.[38] It is also possible to use condensation methods, which have been used to synthesize other Li-benzene structures.[39] Solvent methods may provide more success in creating our modified linkers due to the larger yield compared to molecular beam methods as well as the lower temperatures needed to form the organometallic structures. However, the most promising route may be to synthesize the decorations *in situ*, as recently demonstrated successfully for Li and Na in another MOF.[32]

II. COMPUTATIONAL DETAILS

To study the binding in modified MOF74 we performed *ab initio* calculations at the density functional theory level, as implemented in QUANTUM-ESPRESSO.[40] To account for van der Waals interactions, which play an important role in adsorption in MOFs,[41–44] we employed the newly developed spin-polarized exchange-correlation functional svdW-DF-cx.[45–48] We used norm-conserving pseudopotentials with a plane-wave cutoff of 1088 eV, resulting in a convergence to within 1 meV for energy differ-

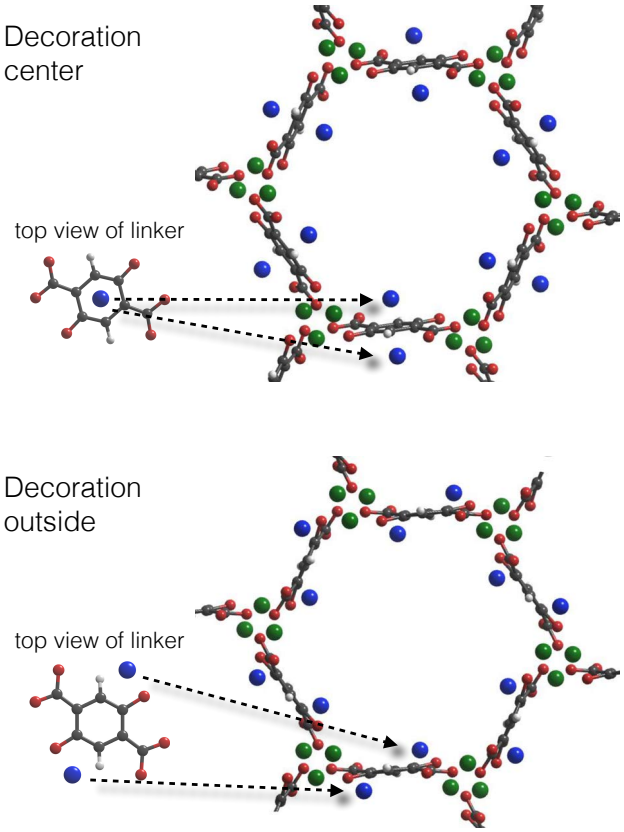

FIG. 1. MOF74 with modified linker 2,5-dihydroxybenzenedicarboxylic acid. (top) Decoration *center*, where one metal atom is attached on each side of the linker, directly above and below the center of the ring. (bottom) Decoration *outside*, where one metal atom is attached on each side of the linker, outside the ring of the linker. Carbon atoms are depicted as grey, oxygen is red, hydrogen is white, and the additional metals are blue. The six original open-metal sites are visible as green in the corners of each channel.

ences. We used Hubbard U corrections for the localized d electrons of Cr, Mn, Fe, Ni, and Cu with the corresponding U values of 3.5, 4, 4, 6.4, and 4 eV.[41,49,50] Mg-MOF74 has a primitive rhombohedral unit cell with space group $R\bar{3}$ and 54 atoms; starting from the experimental atom positions and lattice parameters of $a = 15.117$ Å and $\alpha = 117.742°$,[6,51] we added metals and guest molecules as appropriate, relaxing all geometries until the forces on all atoms were less than 5 meV/Å. As a result of our relaxation, bond lengths differ from the experimental structure on average by approximately 2% (with a standard deviation of less than 1%). As even our highest loading of hydrogen generated only negligible pressure, further relaxations of the unit cell parameters upon loading were not necessary. *Ab initio* Car-Parrinello molecular dynamics (CPMD) simulations were performed with the CP code of QUANTUM-ESPRESSO,[40] using a fictitious electron mass of 400 a.u. and a time step of 5 a.u. The simulations ran for 20 ps, the first ps of which was used for thermalization.

TABLE I. Binding energy ΔE [eV per metal atom] of the various metals $\mathcal{M}$ to the MOF at decoration *center* (c) and *outside* (o), see Fig. 1. $\Delta E_{\text{cluster}}$ [eV per metal atom] indicates how much more favorable the binding to the decoration is compared to forming a small metal cluster.

$\mathcal{M}$	ΔE^c	$\Delta E^c_{\text{cluster}}$	ΔE^o	$\Delta E^o_{\text{cluster}}$
Li	−1.313	−0.423	−1.834	−0.944
Na	−0.824	−0.269	−1.166	−0.611
K	−1.179	−0.726	−1.517	−1.064
Sc	−2.324	−1.316	−2.163	−1.155

III. RESULTS AND DISCUSSION

A. Metal Screening

In order to pre-screen the long list of possible metals mentioned above for our two decorations, we calculated their binding energies to the linker, particularly focusing on the *center* decoration depicted in Fig. 1. Note that this decoration is also stable in the gas-phase linker with nearly identical binding energies and we will use this fact later to estimate the favorable influence of the MOF environment on small-molecule adsorption; decoration *outside* only exists in the MOF and is not stable in the gas-phase linker, as the metal atom is located between the linker and its nearest periodic replica. In our pre-screening we found that Cr, Ni, Cu, Zn, and Ag do not bind. In addition, we found that Pd and Pt result in a very strong binding and warping of the linker, as those atoms bind closer to a carbon of the ring; we do not consider those metals either. Finally, we find that the heavy elements Mn, Fe, and Rb also bind favorably to the linker. However, *a priori*, it was not clear which ones will bind well, so we considered them all. Now, that we have already found several light metals that bind favorably, to keep the gravimetric storage density high we focus on the shortened list of $\mathcal{M}$ = Li, Na, K, and Sc; the binding energies of those metals are listed in Table I. Binding energies are generally strong and on the order of eV. For Li, Na, and K decoration *outside* shows stronger binding compared to decoration *center*. However, part of that difference is alleviated when guest molecules bind more favorable to the *center* decoration, as described below. As such, we expect that under practical circumstances a mixture of both decorations might occur. In addition, we give in Table I values for $\Delta E_{\text{cluster}}$, which show the energy difference of forming the six decorations via binding to the MOF linkers versus binding to themselves and forming a small six-atom metal cluster; all numbers are negative, indicating that the decorations are stable with respect to cluster formation.

The binding characteristics of the various metals can be further analyzed and Table II reports the distances at which the metal $\mathcal{M}$ binds to the MOF as well as the Bader charge[53,54] associated with that metal after ad-

TABLE II. Atomic radii r [Å],[52] binding distances d [Å], and calculated Bader charges q [in units of e, showing electron loss relative to the neutral unit] for each $\mathcal{M}$ at decoration *center* (c) and *outside* (o). For c the distance is measured to the center of the linker ring ($d^c_{\mathcal{M}-\mathrm{C}_6}$) and for o it is measured to the nearest oxygen ($d^o_{\mathcal{M}-\mathrm{O}}$).

$\mathcal{M}$	r	$d^c_{\mathcal{M}-\mathrm{C}_6}$	q^c	$d^o_{\mathcal{M}-\mathrm{O}}$	q^o
Li	1.67	1.65	0.84	1.84	0.89
Na	1.90	2.37	0.52	2.43	0.88
K	2.43	2.56	0.58	2.71	0.83
Sc	1.84	2.19	0.61	2.33	0.78

TABLE III. Binding energy ΔE [eV per guest molecule] of one H_2, CO_2, and H_2O molecule to each metal of decoration *center* (c) and *outside* (o). In comparison, the corresponding binding energies of those molecules at the open-metal sites are −0.15, −0.50, and −0.79 eV, respectively.[42]

$\mathcal{M}$	H_2		CO_2		H_2O	
	ΔE^c	ΔE^o	ΔE^c	ΔE^o	ΔE^c	ΔE^o
Li	−0.240	−0.218	−0.620	−1.336	−1.018	−0.956
Na	−0.080	−0.190	−0.655	−1.941	−0.899	−0.975
K	−0.240	−0.131	−0.668	−2.084	−0.967	−0.891
Sc	+0.096	−0.077	−1.061	−2.342	−0.981	−1.130

TABLE IV. Same as Table III, except that the open-metal sites at the corners are now in addition occupied with a guest molecule of the same kind. There are 12 guest molecules, 6 at the open-metal sites and 6 at the decorations.

$\mathcal{M}$	H_2		CO_2		H_2O	
	ΔE^c	ΔE^o	ΔE^c	ΔE^o	ΔE^c	ΔE^o
Li	−0.191	−0.178	−1.200	−0.942	−1.058	−1.058
Na	−0.081	−0.166	−0.862	−0.756	−0.970	−0.949
K	−0.196	−0.175	−1.044	−0.871	−0.981	−0.885
Sc	−0.046	−0.183	−1.511	−1.768	−0.898	−1.159

sorption. While charge partitioning schemes in general are not unique, one can still gain useful, qualitative information. The distance reported for the *center* decoration is the distance from the metal atom to the center of the linker ring; for the *outside* decoration it is the distance from the metal to the closest oxygen atom found at the end of the adjacent linkers (in this case the metal sits in-between two linkers and binds to the two oxygens of those linkers with the same binding distance). As can be seen, these distances correlate very well with the atomic radii—even for Sc, which is different in nature with its single d electron compared to Li, Na, and K with single s electrons. The Bader charges in Table II tell us how many electrons each metal is giving up when binding. The correlation is generally as expected—closer binding distances show more loss of charge—but the relation is not strictly monotonic. Comparing the Bader charges to the binding energies in Table I, we see that it correlates well for the alkali metals on the *center* decoration. However, it also suggests that the binding mechanism is different for the transition metal Sc, as it binds strongly but only gives up little charge. The variation in the Bader charge for the *outside* decoration is significantly less compared to the *center* decoration and correlations to binding distances and energies are thus less clear. Finally, the electron loss of the metal in the *outside* decoration is typically significantly more compared to the *center* decoration, which is a result of the difference in the Pauli electronegativity of the atoms the metal interacts with in both cases, i.e. O (3.44) vs. C (2.55).[56] This also partly explains the typically stronger binding of the *outside* decoration.

It is also interesting to assess the effect of the decoration on the structure of the MOF itself. From our gas-phase simulations (see the Supplemental Material),[55] we know that some metal decorations can deform and warp the gas-phase linker. However, inside the MOF, the linker is structurally stabilized by the surrounding MOF—except in the case of Pd and Pt, as mentioned above. In summary, we find that the decoration at site *center* causes a distortion with an average bond-length change of 1.4% (with a standard deviation of 1.3%); the *outside* decoration causes larger bond-length changes of 2.9% (with a standard deviation of 1.9%). As expected, the distortion is very localized and the largest changes in bond-lengths for decoration *center* occur in the linker ring—where we find bond-length changes around 4%—and for decoration *outside* near the Mg metal sites with almost 5%.

B. Small-Molecule Uptake

We now turn to the effect of the linker decorations on small-molecule uptake. Tables III and IV show the binding energy of H_2, CO_2, and H_2O to our two linker decorations. Zero-point and vibrational-enthalpy corrections at room temperature are typically small for these molecules in MOF74.[42] In Table III we report the binding energy of one guest molecule to each decoration. While we started by pointing each guest molecule away from the decoration and toward the center of the channel, we found that for certain cases (c and o of H_2 bound to Li; o of CO_2 bound to Li, Na, K, and Sc) after optimization the guest molecule binds between the decoration and the open-metal sites in the corners of the channel. This double-binding process allows for a very strong adsorption and in some cases even chemisorption. The relative binding strengths between the *center* and *outside* decoration varies with adsorbate and metal. However, the fact that for CO_2 the *outside* decoration always shows much more favorable binding in Table III is an artifact of this double-binding and is resolved in Table IV, where double-binding was carefully avoided as discussed below. The length of the CO_2 molecule combined with the location

TABLE V. Same as Table II, but in addition we also show the distance $d_{\mathcal{M}-\mathcal{X}}$ from the metal $\mathcal{M}$ to the closest atom of the adsorbate $\mathcal{X}$ for $\mathcal{X} = H_2$, CO_2, and H_2O.

$\mathcal{M}$	$d^c_{\mathcal{M}-C_6}$	$d^c_{\mathcal{M}-\mathcal{X}}$	q^c	$d^o_{\mathcal{M}-O}$	$d^o_{\mathcal{M}-\mathcal{X}}$	q^o
			$\mathcal{X} = H_2$			
Li	1.65	1.97	0.87	1.87	2.18	0.89
Na	2.29	2.60	0.67	2.45	2.92	0.88
K	2.51	3.22	0.79	2.72	2.97	0.85
Sc	2.15	2.35	0.80	2.29	2.30	0.97
			$\mathcal{X} = CO_2$			
Li	1.72	1.97	0.88	1.94	2.01	0.89
Na	2.31	2.33	0.87	2.51	2.21	0.89
K	2.56	2.77	0.84	3.46	2.65	0.88
Sc	2.15	2.40	1.41	2.25	2.17	1.50
			$\mathcal{X} = H_2O$			
Li	1.76	1.87	0.88	1.93	1.92	0.89
Na	2.44	2.45	0.85	1.93	2.33	0.90
K	2.64	2.83	0.83	2.89	2.84	0.85
Sc	2.24	2.35	0.90	2.26	2.31	0.94

of the metal in the *outside* decoration (see Fig. 1) makes this arrangement very susceptible to double-binding.

Comparing the binding energies in Tables III an IV to the original binding energies of H_2, CO_2, and H_2O at the open-metal sites of -0.15, -0.50, and -0.79 eV,[42] we see that we have created very attractive new binding sites. Note that H_2 in the Sc case does not bind to the *center* decoration, as indicated by the positive binding energy.

The binding of the various guest molecules has been further analyzed in Table V, where we show the corresponding binding distances and Bader charges after adsorption. Comparing with Table II, the change in $d^c_{\mathcal{M}-C_6}$ and $d^o_{\mathcal{M}-O}$ upon adsorption of the guest molecule shows no simple trend. However, the case of H_2 on Li is important for the discussion in Sec. III D, so we point out here that the adsorption of H_2 elongates the metal–MOF bond (and thus weakens it) more so for the *outside* decoration compared to the *center* one. Also, as expected, upon adsorption in all cases the electron loss of the metal increases, as some electron density is now also used for binding the guest molecule. This effect is more noticeable for the *center* decoration. Furthermore, the electron loss of the metal generally follows to following behavior: It starts with a value of approximately 0.88 e for Li, then this value drops and reaches its lowest value either for Na or K, to then finally reach its highest value for Sc. At least for the alkali metals, comparing Table II and V, the *change* in q upon adsorption increases from Li to Na and K, as suggested by the electronegativities of the metals.[56] However, Sc—with its $3d$ electron—does not adhere to that pattern. Finally, the distance from the metal to the guest molecule $d_{\mathcal{M}-\mathcal{X}}$ does consistently follow the pattern of atomic radii in Table II.

TABLE VI. Average binding energy per guest molecule ΔE_{avg} [eV] and incremental binding energy ΔE_{inc} [eV], i.e. the increase in binding energy upon adsorption of each additional guest molecule, for the binding of n H_2 molecules at the *center* (c) and *outside* (o) decorations. The open-metal sites are occupied with one H_2 molecule to prevent double binding.

n	ΔE^c_{avg}	ΔE^c_{inc}	ΔE^o_{avg}	ΔE^o_{inc}
1	-0.191	-0.191	-0.178	-0.178
2	-0.187	-0.179	-0.165	-0.139
3	-0.166	-0.101	-0.155	-0.126
4	-0.155	-0.114	-0.145	-0.106

The double-binding of one guest molecule to a decoration and the open-metal site at the same time does not increase the number of binding sites and is undesirable for our purpose. This does not happen if we increase the guest molecule partial pressure such that the open-metal sites are also occupied with another guest molecule. We report in Table IV the average binding energy of a guest molecule to the decoration while another guest molecule of the same kind is adsorbed at the open-metal sites at the corners. In this scenario, there are 12 guest molecules in the unit cell, six at a decoration and six at the open metal sites. Note that for this partial pressure of guest molecules, this is the ground state for almost all cases in Table IV.[57] In other words, it is typically energetically favorable at higher loadings to bind more guest molecules (both at open-metal sites and decorations) rather than binding some of them strongly through double-binding and not binding the others at all. As an example, looking at the Li *center* decoration with H_2 loading: With 12 H_2 molecules in the unit cell we can either bind 6 of them strongly through double-binding, leaving no open binding sites for the remaining 6, who thus remain unbound. This results in an overall binding energy of $-0.240 \times 6 = -1.44$ eV (see Table III). On the other hand, we can break the double-binding and allow all 12 H_2 molecules to bind, resulting in a much more favorable overall binding energy of $-0.191 \times 12 = -2.29$ eV (see Table IV), which thus becomes the ground state at higher hydrogen partial pressure.

Tables III and IV show that we have truly created additional, attractive binding sites, doubling the number of binding sites compared to the unmodified system. It is also interesting to see that in several instances CO_2 binds more strongly than water—a well sought-after property for effective carbon-capturing applications.[43] In general, binding energies and distances of our Li-decorated linker and adsorbed hydrogen are comparable to *ab initio* studies on metallized graphene,[58,59] aromatic carbon compounds,[60] alkali-metal doped carbon nanotubes,[18] organolithium nanostructures[15] and other Li-decorated MOFs,[20–22,29,61] see the Supplemental Material.[55]

C. High-Loading Case of Hydrogen

Up to now, we have only attached one guest molecule per decoration. However, it has been shown that similar decorations can bind more than one guest molecule.[15,17–21,29,58,59,61] We now seek to bind several guest molecules per decoration and thus maximize the overall molecule uptake. To keep the gravimetric storage density high, we focus on the Li decoration only and study as an example the binding of several H_2 molecules. Table VI shows the average binding energy per guest molecule ΔE_{avg} and the incremental binding energy ΔE_{inc}, i.e. the increase in binding energy upon adsorption of each additional guest molecule; binding geometries are depicted in the Supplemental Material.[55] It is immediately apparent that the Li decoration can bind up to four H_2 molecules with strength similar to the −0.15 eV of the open-metal site.[42] Of particular interest is the incremental binding energy, showing that each additional H_2 molecule still binds with a significant binding energy. Although, as expected, the incremental binding energy decreases with an increase of bound H_2 molecules, it is still very favorable even for four H_2. The system thus favorably binds up to 24 additional guest molecules, i.e. 4 molecules each at the 6 added Li decorations, in addition to the 6 H_2 molecules at the open-metal sites. Interestingly, when loading the MOF with 24 additional hydrogen molecules, the calculated pressure increases only insignificantly in comparison to the empty MOF. Throughout the loading we also noticed that the distance from the Li decoration to the linker ring changes from 1.65 Å (no loading) to 1.69 Å (full loading), see Table I in the Supplemental Material;[55] other structural impacts of the loading are negligible and bond lengths change only on the order of 0.5 % on average. We also studied situations with more than four additional H_2 molecules per Li decoration, but the incremental binding energy becomes less favorable and eventually the system also develops a small but noticeable pressure.

As expected, for both decorations the incremental binding energy decreases with the addition of more H_2—with the exception of three H_2 on the *center* decoration. Looking at the Table II in the Supplemental Material sheds light on this peculiarity.[55] For low loading (one and two H_2) the hydrogen molecules for both decorations stay close to either the original metal site or the new Li site, so that there is always an interaction with a nearby metal. However, when adding the third H_2, we see that in the *center* decoration some molecules are pushed towards the middle of the channel and are very loosely bound without any direct metal interaction, resulting in the low incremental binding energy in this case. Note that this is not the case for the *outside* decoration, where the asymmetry of the Li site provides for more room. Looking at the last row of that table, we see that now six H_2 molecules are pushed towards the middle of the channel—they now gain lateral interactions with each other, which more than compensates for the loss of interactions with nearby metals and increases the incremental binding energy again.

It is interesting to compare the binding to the *center* decoration in the MOF and gas-phase linker;[62] all binding geometries/energies are given in the Supplemental Material.[55] We find that even the gas-phase linker can favorably bind four H_2 molecules. In the MOF cavity however, the binding is more interesting. While the first three H_2 molecules can be said to bind to the decoration, the fourth molecule binds with −0.114 eV towards the center of the channel (see Table VI and Supplemental Material),[55] significantly stronger than the −0.080 eV to the gas-phase linker. It is thus the MOF cavity, together with the decoration and lateral interactions with other hydrogen molecules, that create this favorable binding for the fourth molecule. To verify this effect, we also performed simulations with the same number of hydrogen molecules, but without the decoration, and find that the incremental binding energy of the fourth molecule is only −0.058 eV.

The unmodified Mg-MOF74, assuming one H_2 molecule per open-metal site, has a gravimetric hydrogen storage density of 1.63 mass%. When adding the Li decoration with n H_2 molecules attached to it, this number increases to 3.05 ($n = 1$), 4.50 ($n = 2$), 5.91 ($n = 3$), and 7.28 mass% ($n = 4$). The volumetric density also increases drastically—the unmodified Mg-MOF74 has a value of 15.10 g H_2 L^{-1} for six H_2 molecules located at the six open-metal sites—and our Li decorations with additional 4 H_2 molecules per site reaches even 75.50 g H_2 L^{-1}, i.e. a 5-fold increase.

D. Finite Temperature Behavior

To investigate the hydrogen uptake and stability of our proposed Li decorations in real-world situations, we study them at 1 bar and 77 K, 200 K, and 298 K using *ab initio* CPMD simulations. We model the high-loading regime with one H_2 molecule at each open-metal site and 4 H_2 molecules at each Li decoration. In Fig. 2 we plot the corresponding Li–H radial distribution functions $g_{\text{Li–H}}(r)$. For the *center* decoration we see that the arrangement is stable up to room temperature. At 77 K the integral of the first peak shows that there are 3.1 H_2 molecules in the immediate proximity of the Li. The small peak at 3 Å corresponds to the hydrogens in the linker and is thus not of interest. The peak around 4 Å corresponds to the H_2 molecules from the nearest neighbor Mg metal sites as well as an additional H_2 molecule towards the center of the pore. Once we reach the peak around 5 Å, we start to encounter H_2 molecules from other Li adsorption sites, and by the time we reach the peak around 8 Å and 11 Å, we have hit all the H_2 molecules inside the pore as well as some from surrounding pores. At higher temperatures, the first peak still integrates to 2.75 H_2 molecules. But, the remaining hydrogen molecules—due to thermal fluctuations—distribute

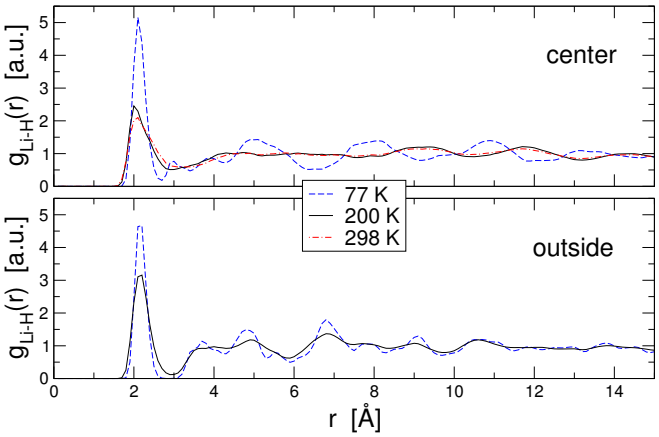

FIG. 2. Li–H radial distribution functions $g_{\mathrm{Li–H}}(r)$ for the *center* and *outside* decorations at 1 bar and temperatures of 77 K, 200 K, and 298 K. The 298 K radial distribution function for the *outside* decoration is not shown, as this decoration becomes unstable at that temperature.

now more evenly across the pore and the radial distribution function flattens at around 4 Å. However, the loss of structure in $g_{\mathrm{Li–H}}(r)$ does not indicate that the hydrogen molecules are not bound—we know from the incremental binding energy in Table VI that all H_2 molecules bind favorably to the system with significant binding energy.

A similar analysis can be done for the *outside* decoration. The main difference, however, is that this decoration is not stable at room temperature and throughout the simulation at that temperature we observe Li detaching from the linker. At first, this result seems surprising, as Table I shows that Li is bound to the linker considerably stronger in this scenario and one would expect that the *center* decoration becomes unstable before the *outside* one does. However, that table only shows the binding of Li by itself and increased loading with H_2 weakens that binding in different ways for both decorations. Comparing Table II and V we see that adsorption of H_2 has no noticeable effect on the metal–MOF bond in case of the *center* decoration, where $d^c_{\mathcal{M}-\mathrm{C}_6}$ remains unchanged. On the other hand, for the *outside* decoration the adsorption of already one hydrogen molecule leads to a noticeable elongation of the bond length $d^o_{\mathcal{M}-\mathrm{O}}$, indicating a weakening of that bond and explaining why the *outside* decoration becomes unstable before the *center* one does under high hydrogen loading conditions.

IV. CONCLUSIONS

In summary, we propose linker decorations for MOF74, i.e. the binding of a metal above and below the linker's ring, to create new strong adsorption sites. We show that this simple decoration increases the small-molecule uptake significantly, as each of them can bind several additional guest molecules. When using Li to create new adsorption sites, we find that its binding of guest molecules is comparable in strength to the already existing open-metal sites. For the case of hydrogen storage, we find further that up to four additional hydrogen molecules can be adsorbed per Li site, increasing the hydrogen uptake by a factor of 5.

ACKNOWLEDGMENTS

CAA and SZ were supported by DOE Grant No. DE–FG02–08ER46491 and were responsible for all MOF aspects of this study. DH an EW were supported by NSF Grant No. DMR–1145968 and supported all hydrogen storage aspects of this study.

* E-mail: thonhauser@wfu.edu

[1] L. J. Murray, M. Dinca, and J. R. Long, Chem. Soc. Rev. **38**, 1294 (2009).
[2] J.-R. Li, Y. Ma, M. C. McCarthy, J. Sculley, J. Yu, H.-K. Jeong, P. B. Balbuena, and H.-C. Zhou, Coord. Chem. Rev. **255**, 1791 (2011).
[3] S. Qiu and G. Zhu, Coord. Chem. Rev. **253**, 2891 (2009).
[4] D. Zhao, D. Yuan, and H.-C. Zhou, Energy Environ. Sci. **1**, 222 (2008).
[5] N. L. Rosi, J. Eckert, M. Eddaoudi, D. T. Vodak, J. Kim, M. O'Keeffe, and O. M. Yaghi, Science **300**, 1127 (2003).
[6] H. Wu, J. M. Simmons, G. Srinivas, W. Zhou, and T. Yildirim, J. Phys. Chem. Lett. **1**, 1946 (2010).
[7] P. D. C. Dietzel, R. E. Johnsen, H. Fjellvag, S. Bordiga, E. Groppo, S. Chavan, and R. Blom, Chem. Commun. , 5125 (2008).
[8] S. R. Caskey, A. G. Wong-Foy, and A. J. Matzger, J. Am. Chem. Soc. **130**, 10870 (2008).
[9] J. Liu, P. K. Thallapally, B. P. McGrail, D. R. Brown, and J. Liu, Chem. Soc. Rev. **41**, 2308 (2012).
[10] L. E. Kreno, K. Leong, O. K. Farha, M. Allendorf, R. P. Van Duyne, and J. T. Hupp, Chem. Rev. **112**, 1105 (2012).
[11] See, e.g. `http://www.hydrogen.energy.gov/annual_review12_proceedings.html`.
[12] D. Harrison, E. Welchman, Y. J. Chabal, and T. Thonhauser, in *Vol. 5 Energy Storage, Handbook of Clean Energy Systems*, edited by J. Yan (Wiley, Hoboken, NJ, 2015) pp. 2665–2683.
[13] M. G. Lopez, P. Canepa, and T. Thonhauser, J. Chem. Phys. **138**, 154704 (2013).
[14] M. C. Das, S. Xiang, Z. Zhang, and B. Chen, Angew. Chem. Int. Ed. **50**, 10510 (2011).
[15] S. Namilae, M. Fuentes-Cabrera, B. Radhakrishnan, G. Sarma, and D. Nicholson, Chem. Phys. Lett. **436**, 150 (2007).
[16] R. C. Lochan and M. Head-Gordon, Phys. Chem. Chem. Phys. **8**, 1357 (2006).

[17] Q. Sun, P. Jena, Q. Wang, and M. Marquez, J. Am. Chem. Soc. **128**, 9741 (2006).
[18] G. E. Froudakis, Nano Letters **1**, 531 (2001).
[19] A. Li, R.-F. Lu, Y. Wang, X. Wang, K.-L. Han, and W.-Q. Deng, Angew. Chem. Int. Ed. **49**, 3330 (2010).
[20] A. Blomqvist, C. Moysés Araújo, P. Srepusharawoot, and R. Ahuja, PNAS **104**, 20173 (2007).
[21] P. Srepusharawoot, A. Blomqvist, C. M. Araújo, R. H. Scheicher, and R. Ahuja, Int. J. Hydrogen Energy **36**, 555 (2011).
[22] P. Srepusharawoot, E. Swatsitang, V. Amornkitbamrung, U. Pinsook, and R. Ahuja, Int. J. Hydrogen Energy **38**, 14276 (2013).
[23] K. L. Mulfort and J. T. Hupp, J. Am. Chem. Soc. **129**, 9604 (2007).
[24] E. D. Bloch, D. Britt, C. Lee, C. J. Doonan, F. J. Uribe-Romo, H. Furukawa, J. R. Long, and O. M. Yaghi, J. Am. Chem. Soc. **132**, 14382 (2010).
[25] M. Dincä and J. R. Long, Angew. Chem. Int. Ed. **47**, 6766 (2008).
[26] K. L. Mulfort, O. K. Farha, C. L. Stern, A. A. Sarjeant, and J. T. Hupp, J. Am. Chem. Soc. **131**, 3866 (2009).
[27] D. Himsl, D. Wallacher, and M. Hartmann, Angew. Chem. Int. Ed. **48**, 4639 (2009).
[28] D. Rao, R. Lu, C. Xiao, E. Kan, and K. Deng, Chem. Comm. **47**, 7698 (2011).
[29] K. Srinivasu and S. K. Ghosh, J. Phys. Chem. C **115**, 16984 (2011).
[30] P. Dalach, H. Frost, R. Q. Snurr, and D. E. Ellis, J. Phys. Chem. C **112**, 9278 (2008).
[31] Z. Xiang, Z. Hu, D. Cao, W. Yang, J. Lu, B. Han, and W. Wang, Angew. Chem. Int. Ed. **50**, 491 (2011).
[32] M. Anbia and M. Faryadras, J. Nanostructure Chem. **5**, 357 (2015).
[33] R. Pandey, B. K. Rao, P. Jena, and M. A. Blanco, J. Am. Chem. Soc. **123**, 3799 (2001).
[34] C. W. Bauschlicher Jr, H. Partridge, and S. R. Langhoff, J. Phys. Chem. **96**, 3273 (1992).
[35] J. Granatier, P. Lazar, M. Otyepka, and P. Hobza, J. Chem. Theory Comput. **7**, 3743 (2011).
[36] J. Granatier, M. Dubecký, P. Lazar, M. Otyepka, and P. Hobza, J. Chem. Theory Comput. **9**, 1461 (2013).
[37] I. S. Youn, D. Y. Kim, N. J. Singh, S. W. Park, J. Youn, and K. S. Kim, J. Chem. Theory Comput. **8**, 99 (2012).
[38] T. Kurikawa, H. Takeda, M. Hirano, K. Judai, T. Arita, S. Nagao, A. Nakajima, and K. Kaya, Organometallics **18**, 1430 (1999).
[39] L. Manceron and L. Andrews, J. Am. Chem. Soc. **110**, 3840 (1988).
[40] P. Giannozzi, S. Baroni, N. Bonini, M. Calandra, R. Car, C. Cavazzoni, D. Ceresoli, G. L. Chiarotti, M. Cococcioni, I. Dabo, A. Dal Corso, S. de Gironcoli, S. Fabris, G. Fratesi, R. Gebauer, U. Gerstmann, C. Gougoussis, A. Kokalj, M. Lazzeri, L. Martin-Samos, N. Marzari, F. Mauri, R. Mazzarello, S. Paolini, A. Pasquarello, L. Paulatto, C. Sbraccia, S. Scandolo, G. Sclauzero, A. P. Seitsonen, A. Smogunov, P. Umari, and R. M. Wentzcovitch, J. Phys. Condens. Matter **21**, 395502 (2009).
[41] K. Lee, J. D. Howe, L.-C. Lin, B. Smit, and J. B. Neaton, Chem. Mater. **27**, 668 (2015).
[42] P. Canepa, N. Nijem, Y. J. Chabal, and T. Thonhauser, Phys. Rev. Lett. **110**, 026102 (2013).
[43] P. Canepa, C. A. Arter, E. M. Conwill, D. H. Johnson, B. A. Shoemaker, K. Z. Soliman, and T. Thonhauser, J. Mater. Chem. A **1**, 13597 (2013).
[44] K. Tan, S. Zuluaga, Q. Gong, P. Canepa, H. Wang, J. Li, Y. J. Chabal, and T. Thonhauser, Chem. Mater. **26**, 6886 (2014).
[45] T. Thonhauser, S. Zuluaga, C. A. Arter, K. Berland, E. Schröder, and P. Hyldgaard, Phys. Rev. Lett. **115**, 136402 (2015).
[46] K. Berland, V. R. Cooper, K. Lee, E. Schröder, T. Thonhauser, P. Hyldgaard, and B. I. Lundqvist, Reports Prog. Phys. **78**, 066501 (2015).
[47] T. Thonhauser, V. R. Cooper, S. Li, A. Puzder, P. Hyldgaard, and D. C. Langreth, Phys. Rev. B **76**, 125112 (2007).
[48] D. C. Langreth, B. I. Lundqvist, S. D. Chakarova-Käck, V. R. Cooper, M. Dion, P. Hyldgaard, A. Kelkkanen, J. Kleis, L. Kong, S. Li, P. G. Moses, E. D. Murray, A. Puzder, H. Rydberg, E. Schröder, and T. Thonhauser, J. Phys. Condens. Matter **21**, 084203 (2009).
[49] L. Wang, T. Maxisch, and G. Ceder, Phys. Rev. B **73**, 195107 (2006).
[50] R. Poloni, K. Lee, R. F. Berger, B. Smit, and J. B. Neaton, J. Phys. Chem. Lett. **5**, 861 (2014).
[51] H. Wu, W. Zhou, and T. Yildirim, J. Am. Chem. Soc. **131**, 4995 (2009).
[52] E. Clementi and D. L. Raimondi, J. Chem. Phys. **38**, 2686 (1963).
[53] R. F. W. Bader, *Atoms in Molecules: A Quantum Theory* (Oxford University Press, New York, 1990).
[54] G. Henkelman, A. Arnaldsson, and H. Jónsson, Comp. Mater. Science **36**, 354 (2006).
[55] See Supplemental Material at ... for a comparison with other computational studies, binding geometries, and further results from simulations on the gas-phase linker.
[56] A. L. Allred, J. Inorg. Nucl. Chem. **17**, 215 (1961).
[57] CO_2 binding to a Na and K *outside* decoration is an exception, where double-binding is the ground state even for higher partial CO_2 pressures.
[58] W. Zhou, J. Zhou, J. Shen, C. Ouyang, and S. Shi, J. Phys. Chem. Solids **73**, 245 (2012).
[59] C. Ataca, E. Aktürk, S. Ciraci, and H. Ustunel, Appl. Phys. Lett. **93**, 043123 (2008).
[60] Y. Zhao, R. Zhang, and R. Wang, Chem. Phys. Lett. **398**, 62 (2004).
[61] S. J. Kolmann, B. Chan, and M. J. Jordan, Chem. Phys. Lett. **467**, 126 (2008).
[62] The *outside* decoration is not stable in the gas phase, so the comparison cannot be done in that case.